# Swarm Level 2 Processing System

# Intermediate validation of Swarm Level 2 Core Field Product

**SW_OPER_MCO_SHAi2C_20131126T000000_20160101T000000_0202**

**By: DTU**

**Date: 2016-04-12**

## Abstract and Conclusion

The processes and tests applied in the intermediate validation of the MCO_SHAi2C product

**SW_OPER_MCO_SHAi2C_20131126T000000_20160101T000000_0202**

and the conclusions on the product quality drawn here from are described in this document.

This product contains the representation of a model of the magnetic field of Earth's core and its temporal evolution ("MCO" part of product name) using spherical harmonic coefficients ("SHA" part of product name). The model is estimated from Swarm and observatory data using the *Comprehensive Inversion* (CI) scheme within the Swarm Level 2 Processing system ("2C" part of product name). Operational Swarm Level 1b data version 0408/0409, covering the period from 2013-11-26 to 2015-12-31 are used for the model estimation and the product is valid over the same period ("20131126T000000_20160101T000000" part of product name). This is version 0202 of the product (last part of product name) indicating a significant change in the Comprehensive Inversion process since the previous release and this is the second, minor version of the product. The format of the product is described in "Product Specification for L2 Products and Auxiliary Products", doc. no. SW-DS-DTU-GS-0001.

The assessment of the SW_OPER_MCO_SHAi2C_20131126T000000_20160101T000000_0202 product show very good agreement with recent versions of the CHAOS-6 model and Swarm Initial Field Model [Olsen, N., GRL-42, 2015].

**The DTU SIL's opinion is that the MCO_SHAi2C product is validated and is therefore suitable for release.**

## Table of Contents



## Table of Figures

## Table of Tables



## Abbreviations

| *Acronym* | *Description* |
|---|---|
| CI | Comprehensive Inversion |
| CMB | Core-Mantle Boundary |
| EUL | Euler Angle |
| L2PS | Level 2 Processing System |
| MCO | Magnetic Core field |
| PDGS | Payload Data Ground Segment |
| SHA | Spherical Harmonic Analysis |
| SIL | Scientist in the Loop |
| STR | Star Tracker |
| TDS | Test Data Set |
| VAL | Validation |
| VFM | Vector Field Magnetometer |

# 1 Intermediate Validation Report of MCO_SHAi2C

## 1.1 Input products and data

The following products were used as input for the estimation of the MCO_SHAi2C core field model

| Products | Type | Period | Comment |
|---|---|---|---|
| SW_OPER_Q3D_CI_i2__00000000T000000_99999999T999999_0101 | Q-matrix of Earth's (1_D mantle + oceans) | - | Used for computing induced part of ionospheric field |
| SW_OPER_AUX_OBS_2__20130101T000000_20131231T235959_0104<br>SW_OPER_AUX_OBS_2__20140101T000000_20141231T235959_0104<br>SW_OPER_AUX_OBS_2__20150101T000000_20151231T235959_0104 | Observatory hourly mean values | 2013-11-23 – 2015-07-28 | A total of 121 observatories are included |
| SW_OPER_AUX_DST_2__19980101T013000_20150308T233000_0001<br>SW_OPER_AUX_F10_2__19980101T000000_20150401T000000_0001<br>SW_OPER_AUX_KP__2__19990101T023000_20150228T223000_0001 | Indices | As indicated by the file names | |
| SW_OPER_MAGA_LR_1B_*yyyymmddTh1m1s1_yyyymmddTh2m2s2*_0408<br>SW_OPER_MAGB_LR_1B_*yyyymmddTh1m1s1_yyyymmddTh2m2s2*_0408<br>SW_OPER_MAGC_LR_1B_*yyyymmddTh1m1s1_yyyymmddTh2m2s2*_0409 | Swarm magnetic data, 1 Hz | 2013-11-26 - 2015-12-31 | Decimated to 15 second sampling |

Table 1-1: Input products

## 1.2 Model Parameterization and Data Selection

See Section 2.1.

## 1.3 Output Products

The products of this validation report are:

*Swarm Level 2 Magnetic core field Product:*

SW_OPER_MCO_SHAi2C_20131126T000000_20160101T000000_0202

*Swarm Level 2 Intermediate Validation Product:*

SW_OPER_MCO_VALi2C_20131126T000000_20160101T000000_0202

## 1.4 Validation Results

The tests were conducted between 2016-02-22 and 2016-04-10

The following tests have been applied to the data. See Annex A for general definitions of various tests.

### 1.4.1 Spectral Power Density

Figure 1-1 below shows the spectral power density of the static core field model ("CI", in black, epoch 2015.0) and of the power of the difference between the CI core field model and the CHAOS-6 (blue) and the Swarm Initial Field Model ( "SIFM+" in green) respectively.

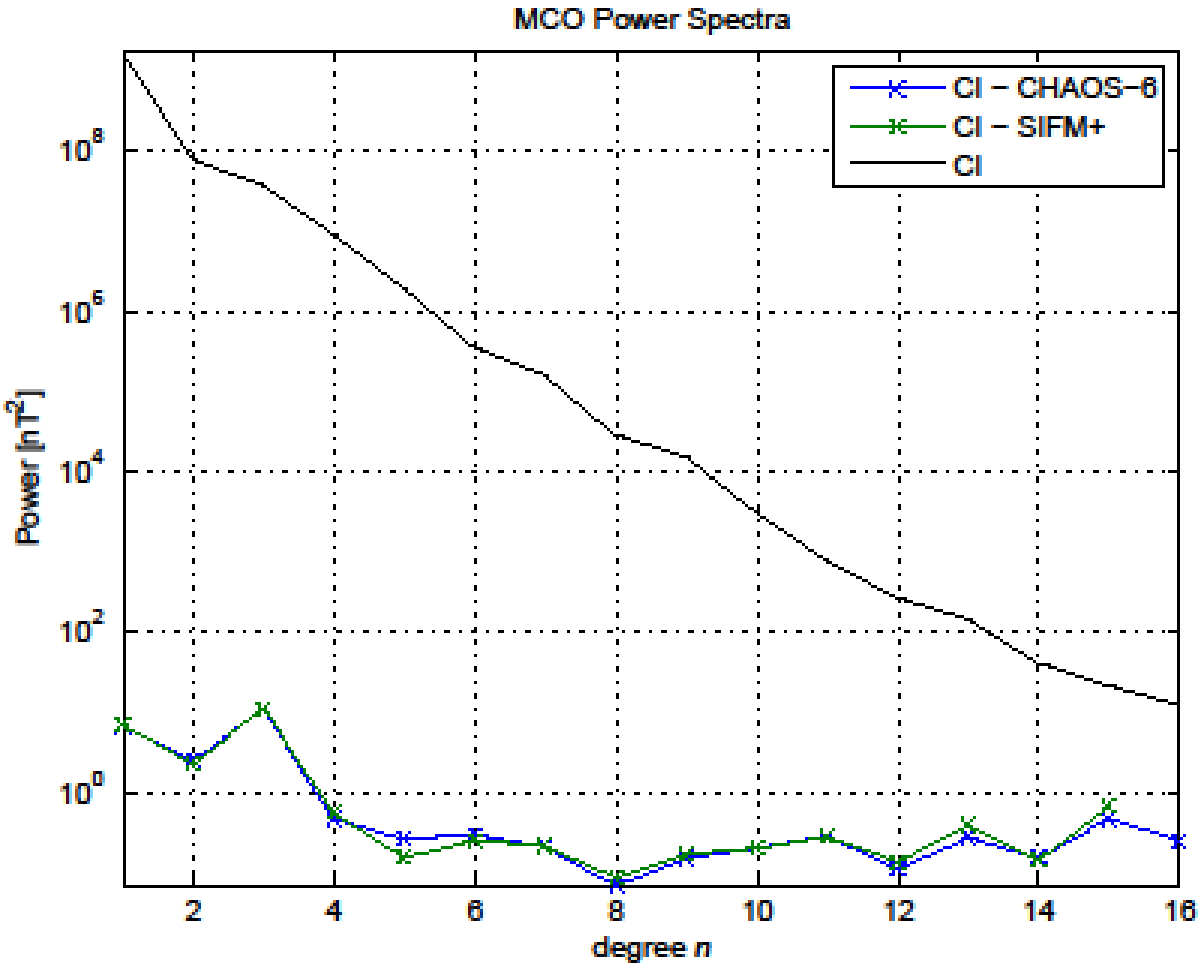


Figure 1-1: Spectral power density, static core field

In Figure 1-2 on the next page are shown the corresponding spectral power density of the first time derivate – the Secular Variation, SV – of the models at epoch 2015.0, plus the CI SV spectral power at epochs 2014.0 and 2016.0.

These plots demonstrate the good agreement between the CI core field product and the CHAOS-6 and Swarm Initial Field Models.

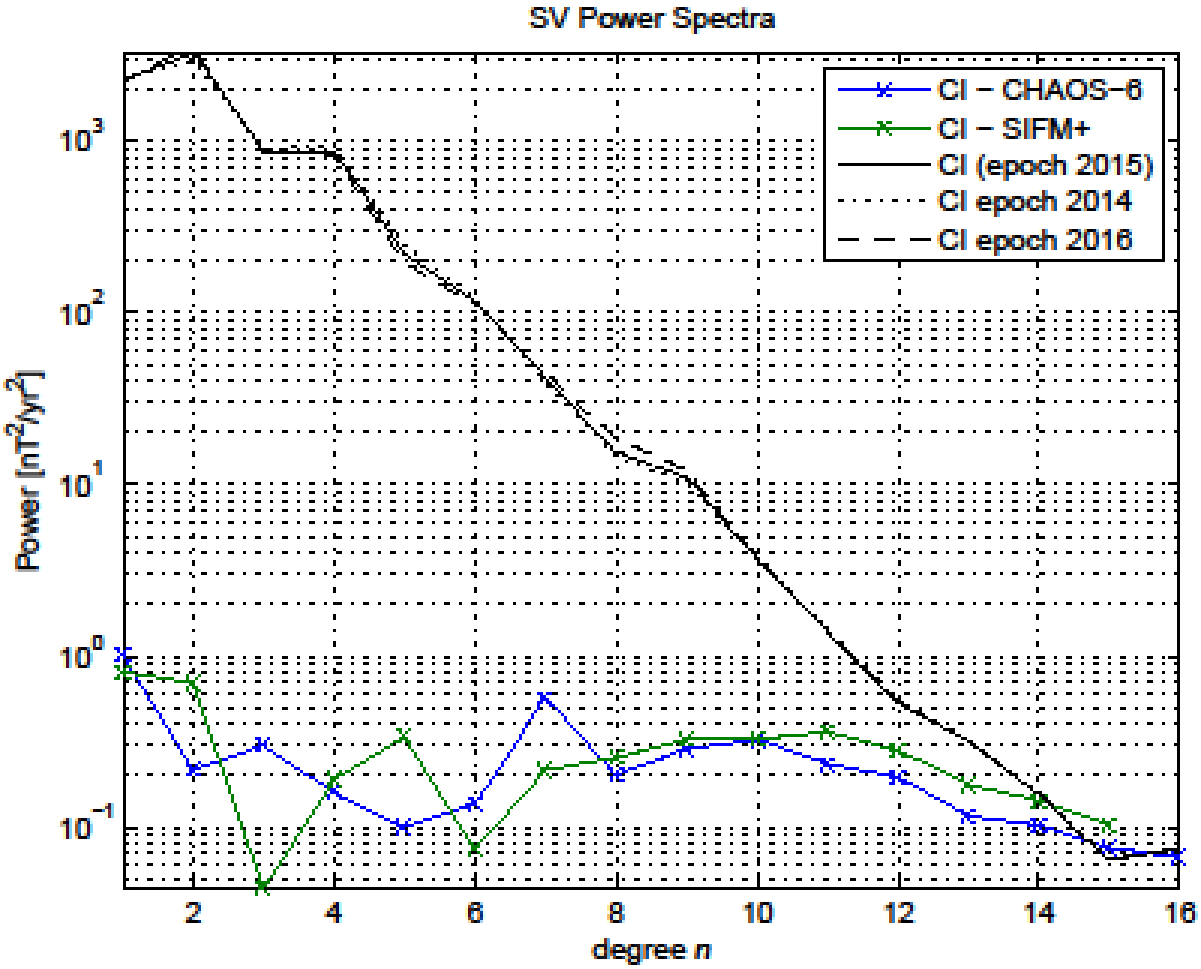


Figure 1-2: Spectral power density, secular variation, main epoch 2015.0

### 1.4.2 Secular Variation per spherical harmonic coefficient

Figure 1-3 below shows timeseries of the first time-derivatives of the spherical harmonic coefficients up to degree 3. The magenta curves show the CI core field model coefficient derivatives and the blue and green curves show the CHAOS-6 and Swarm Initial Field model coefficient derivatives respectively. The figure confirms the good agreement between the three models, although with small differences.

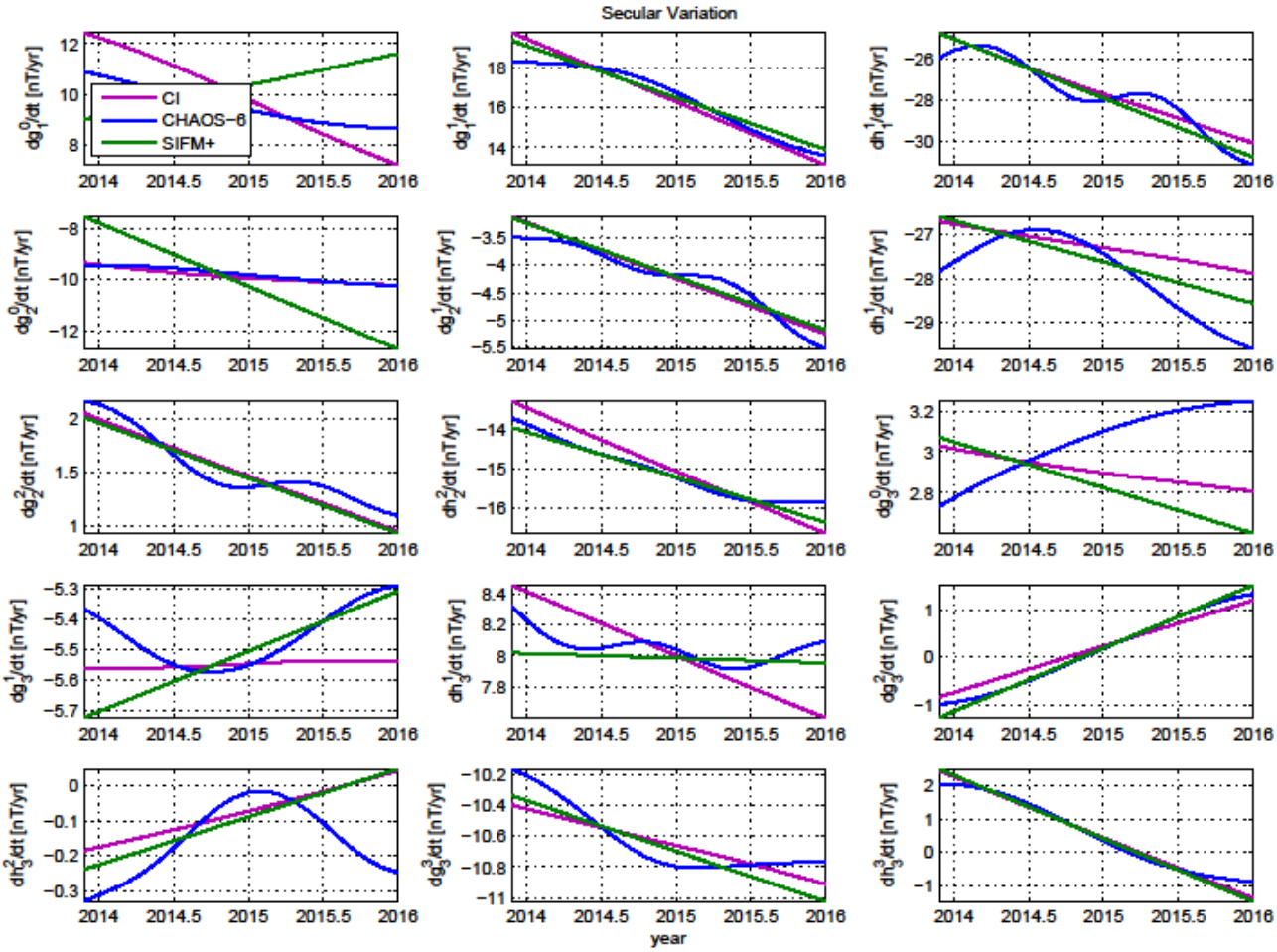


Figure 1-3: Spherical harmonic coefficients, degrees 1-3

### 1.4.3 Secular Variation at Core-Mantle Boundary

Examining the vertical component of the magnetic field at the core-mantle boundary (CMB) reveals some unexpected features which requires caution if the CI core field model is to be used in studies of the CMB. Figure 1-4 below shows the first time-derivative of $B_r$ at the CMB; the large patches in the northern hemisphere (top left) are much stronger than usually seen.

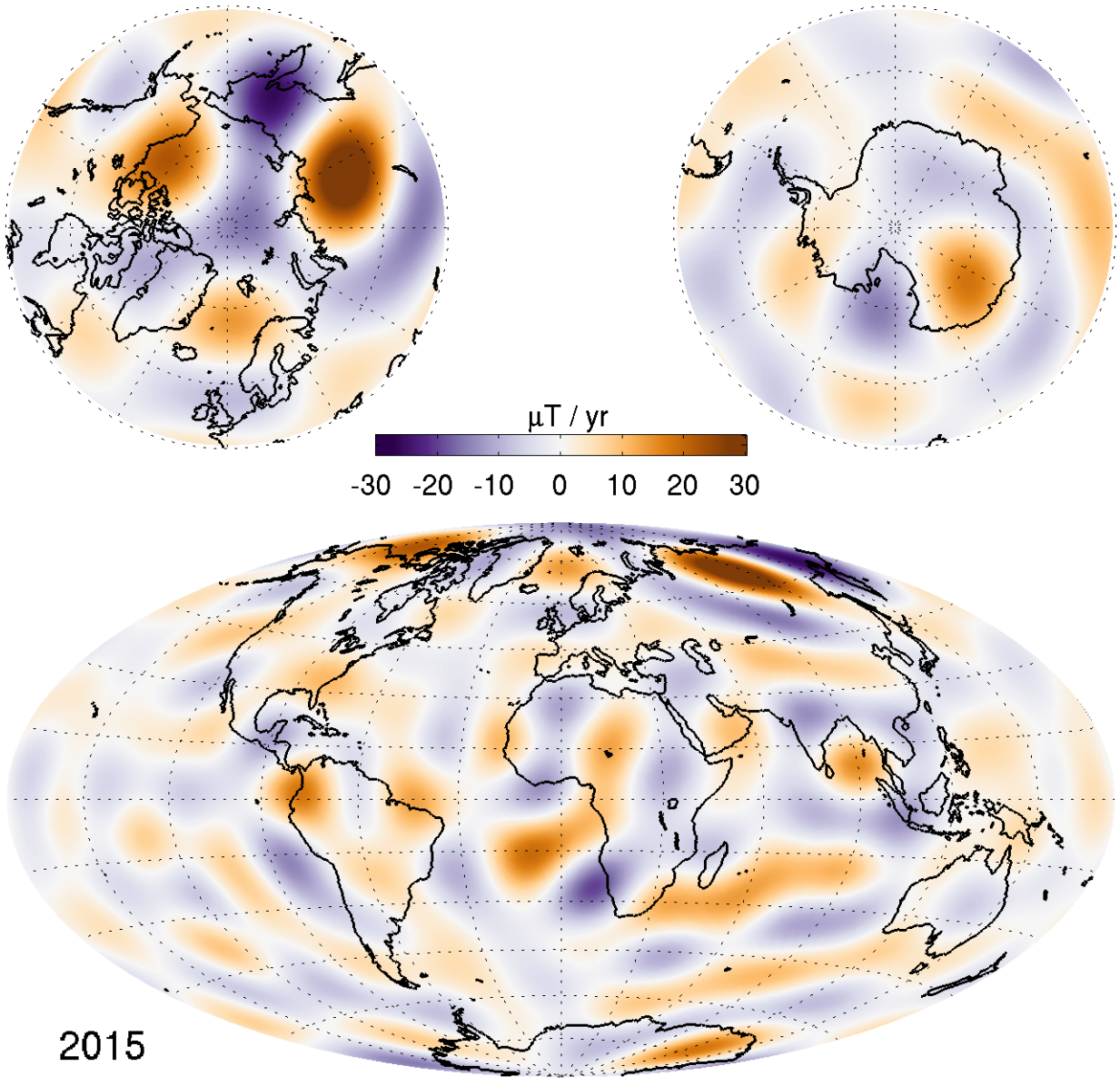


Figure 1-4: Map of $dB_r/dt$ at core-mantle boundary, up to degrees 13

Furthermore, when looking at the second time-derivative of $B_r$, cf. Figure 1-5, significantly larger drifts of the patches are observed.

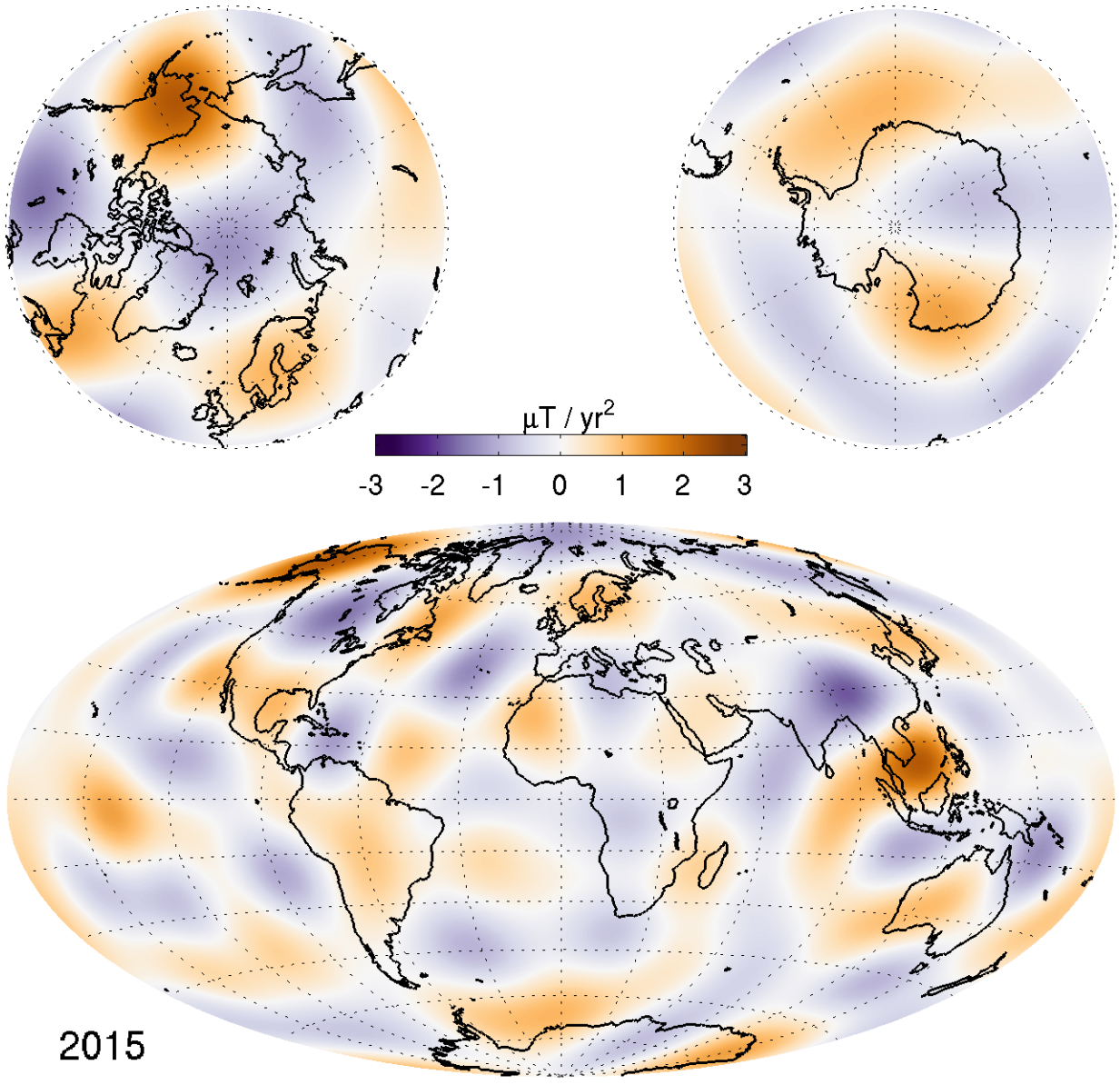


Figure 1-5: Map of $d^2B_r/dt^2$ at core-mantle boundary, up to degrees 13

### 1.4.4 Data Statistics

The statistics of the measurement data obtained by the CI modelling are given in Table 1-2 below. Grey cells indicate data from eclipse, white cells indicate data from sunlit periods. Crossed cells indicate data which are not used in the inversion process. "Field" indicate the pure vector and scalar measurements, whereas "NS diff" and "EW diff" indicate the North-South (along-track) respectively East-West differences. The standard deviations (of the residuals between the observations and the estimated model) are quite impressive, and also show the expected similarity between Swarm A and C (side-by-side flying pair) and in the North-South differences for all ≤three satellites. As also expected, Swarm B shows slightly higher residuals in the Field components at low and mid latitudes due to its higher altitude.

| Swarm/Obs. | | Geomagnetic quasi-dipole latitude | | | | | | | | | | | |
|---|---|---|---|---|---|---|---|---|---|---|---|---|---|
| | | Low, ≤ 10° | | | | Mid, ]10°..55°] | | | | High, > 55° | | | |
| | | Standard deviations of data residuals, weighted, [nT] | | | | | | | | | | | |
| | | $\sigma(B_r)$ | $\sigma(B_\theta)$ | $\sigma(B_\varphi)$ | $\sigma(F)$ | $\sigma(B_r)$ | $\sigma(B_\theta)$ | $\sigma(B_\varphi)$ | $\sigma(F)$ | $\sigma(B_r)$ | $\sigma(B_\theta)$ | $\sigma(B_\varphi)$ | $\sigma(F)$ |
| A | Field | 1.75 | 2.07 | 2.01 | 1.98 | 1.74 | 2.70 | 3.10 | 1.45 | | | | 8.55 |
| | NS diff | 0.39 | 0.19 | 0.40 | 0.16 | 0.25 | 0.31 | 0.39 | 0.16 | | | | 1.70 |
| | | 1.27 | 0.95 | 1.22 | 0.82 | 0.63 | 0.73 | 1.32 | 0.34 | | | | 2.54 |
| B | Field | 2.04 | 3.25 | 2.96 | 3.12 | 2.24 | 3.92 | 4.16 | 2.18 | | | | 8.15 |
| | NS diff | 0.39 | 0.18 | 0.38 | 0.16 | 0.25 | 0.31 | 0.39 | 0.17 | | | | 1.48 |
| | | 1.13 | 0.81 | 1.14 | 0.68 | 0.61 | 0.72 | 1.32 | 0.32 | | | | 2.23 |
| C | Field | 1.79 | 2.06 | 2.04 | 2.01 | 1.75 | 2.72 | 3.10 | 1.47 | | | | 8.56 |
| | NS diff | 0.41 | 0.19 | 0.41 | 0.17 | 0.26 | 0.32 | 0.41 | 0.16 | | | | 1.71 |
| | | 1.27 | 0.95 | 1.23 | 0.81 | 0.63 | 0.74 | 1.33 | 0.34 | | | | 2.54 |
| A-C | EW diff | 0.89 | 0.41 | 1.20 | 0.32 | 0.50 | 0.53 | 1.17 | 0.31 | | | | 0.64 |
| | | 2.18 | 0.81 | 2.86 | 0.57 | 1.93 | 3.41 | 2.35 | 0.47 | | | | 0.78 |
| Magnetic observatories | | 4.60 | 4.38 | 5.74 | 4.74 | 4.20 | 4.83 | 4.83 | 4.26 | 7.31 | 5.98 | 7.57 | 7.38 |
| | | 11.39 | 11.29 | 10.54 | 11.27 | 8.50 | 10.01 | 7.12 | 7.65 | 16.67 | 13.99 | 14.79 | 14.61 |

Table 1-2: Observation Statistics

## 1.5 Criteria

Table 1-3 below summarizes the criteria used to check the validity of the MCO_SHAi2C product.

| Input | Test | Criteria | Pass? |
|---|---|---|---|
| Observations | Residual statistics | Standard deviation of vector data below 7 nT. | Ok |
| Alternative model | Comparison with model | CI model agrees with alternative model | Ok |

Table 1-3: Validation criteria

# 2 Additional Information

## 2.1 Model Configuration and Data Selection Parameters

The MCO_SHAi2C product is obtained as a comprehensive co-estimation of the core, lithosphere, ionosphere, and magnetosphere field contributions including induced contributions. The complete model configuration used is given in Table 2-1 below; the MCO_SHAi2C product is the green part:

| **Model Part** | **Maximum Degree/Order** | **Temporal Characteristics** | **Comment** |
|---|---|---|---|
| Core | 16/16 | Order 4 B-spline with knots every year | Damping of the mean-square, second and third time derivatives of $B_r$ at the core-mantle boundary (at 3480 km radius). The damping makes the secular variation virtually linear as seen in Figure 1-3. |
| Lithosphere | 90/90 | Static | Degree 17-90 purely determined by North-South differences from all satellites and East-West differences of lower pair satellite (A and C).<br><br>Damping of $B_r$ at the poles to reduce potential effect of lack of data at the poles ("*polar gap*") |
| Ionosphere | 45/5 (dipole coordinates) | Annual, semi-annual, 24-, 12-, 8- and 6- hours periodicity | Spherical harmonic expansion in quasi-dipole (QD) frame, underlying dipole SH $n_{max} = 60$, $m_{max} = 12$. F10.7 scaling plus induction via a priori 3-D conductivity model ("1-D+oceans") and infinite conductor at depth.<br><br>Damping of:<br><br>1. Mean-square current density J in the E-region within the nightside sector (magnetic local times 21:00 through 05:00)<br><br>2. Mean-square of the surface Laplacian of J multiplied by a factor of $\sin^8(2\theta)$ over all local times, where $\theta$ is co-latitude. |

| Model Part | Maximum Degree/Order | Temporal Characteristics | Comment |
|---|---|---|---|
| Magnetosphere, external | 3/1 | One hour bins | |
| Magnetosphere, induced | 3/3 | One hour bins | |
| M2 Tidal | 36/36 | Periodicity: 12.42060122 hr, phase fixed with respect to 00:00:00, 1999 January 1 GMT | |

Table 2-1: Model Configuration

The data selection criteria are:

- Coarse agreement with CHAOS-6 field model: $\Delta B_c \leq 500$ nT for all components $c$, and $\Delta F \leq 100$ nT.
- $Kp \leq 2^+$
- Time-derivative of Dst $\leq 3$ nT/hour
- 15 second satellite sampling period
- core and tidal fields determined from night-side data only, i.e. with Sun $\geq 10°$ below the horizon

## 2.2 Comments from Scientists in the Loop

### 2.2.1 Derivation of Model

The final Comprehensive Inversion model for the first two years of Swarm data show good agreement with alternative models and very good statistics (Table 1-2), although some caution must be taken when studying the features at the core-mantle boundary (Section 1.4.3). The estimated ionospheric model may have some minor deficiencies which may also impact the magnetospheric model, this should have no impact on the estimated core and lithospheric field models.

### 2.2.2 Conclusion

The estimated model is assessed to be of good quality with very good agreement with alternative core field models.

# Annex A Definitions of Tests

## A.1 Mean square vector field difference per spherical harmonic degree

The mean square vector field difference between models per spherical harmonic degree ($n$) is diagnostic of how closely the models match on average across the globe. The difference between Gauss coefficients ${}^{m}_{n}g$ of model $i$ and model $j$ can be defined as:

$$ {}_{i,j}R_n = (n+1)\left(\frac{a}{r}\right)^{(2n+4)} \sum_{m=0}^{n}\left[{}_{i}g_n^m - {}_{j}g_n^m\right]^2 $$

Equation A-1

where $n$ is the degree, $m$ is the order, $a$ is the magnetic reference spherical radius of 6371.2 km which is close to the mean Earth radius, and $r$ is the radius of the sphere of interest, which is taken as r = a for comparisons at the Earth's surface and r = 3480 km for comparisons at the core-mantle boundary.

Summing over degrees n from 1 to the truncation degree N and taking the square root yields the RMS vector field difference between the models $i$ and $j$ averaged over the spherical surface:

$$ {}_{i,j}R = \sqrt{\sum_{n=1}^{N} {}_{i,j}R_n} $$

Equation A-2

## A.2 Correlation per spherical harmonic degree

Analysis of spherical harmonic spectra is a powerful way to diagnose differences in amplitude between models but tells us little about how well they are correlated. The correlation per degree between two models again labelled by the indices $i$ and $j$ can be studied as a function of spherical harmonic degree using the quantity: ${}_{i,j}\rho_n$

$$ {}_{i,j}\rho_n = \frac{\sum_{m=0}^{n}\left({}_{i}g_n^m \; {}_{j}g_n^m\right)}{\sqrt{\left(\sum_{m=0}^{n}\left({}_{i}g_n^m\right)^2\right)\left(\sum_{m=0}^{n}\left({}_{j}g_n^m\right)^2\right)}} $$

Equation A-3

Ideally, the correlation should be close to 1 for all models, indicating that they have equivalent features and coefficients. If the correlation falls below 0.5, for degrees 1-9, then the models should be examined in more detail. Coefficients from degree 10-13 in IGRF and WMM are less well-determined (e.g. due to noise) and also change more rapidly so are not expected to be well correlated by the launch of the Swarm mission.

## A.3 Visualisation of coefficient differences

A final method of visualising the differences in Gauss coefficients is to plot the differences ${}_{i}g_n^m - {}_{j}g_n^m$ as a triangular plot, with the zonal coefficients lying along the centre of the triangle, the sectorial coefficients along the edges and the tesseral coefficients filling the central regions. These plots will illustrate which, if any, coefficients are strongly divergent between models.